Collision-induced dissociation of bradykinin ions in the interface region of an ESI-MS

ARTICLE *in* JOURNAL OF THE AMERICAN SOCIETY FOR MASS SPECTROMETRY · AUGUST 2001

Impact Factor: 2.95 · DOI: 10.1016/S1044-0305(01)00266-5 · Source: PubMed

3 AUTHORS, INCLUDING:

Bradley B Schneider
SCIEX
39 PUBLICATIONS **1,054** CITATIONS
SEE PROFILE

David Chen
University of British Columbia - Vancouver
112 PUBLICATIONS **3,578** CITATIONS
SEE PROFILE

Collision-Induced Dissociation of Bradykinin Ions in the Interface Region of an ESI-MS

Bradley B. Schneider, D. J. Douglas, and David D. Y. Chen
Department of Chemistry, University of British Columbia, Vancouver, British Columbia, Canada

By applying different electric field strengths to the orifice–skimmer region of an electrospray ionization mass spectrometer, the rate of dissociation can be varied based on the amount of internal energy acquired by an ion through collisions with the curtain gas molecules. Both the Arrhenius equation and Rice-Ramsperger-Kassel (RRK) theory can be used to predict the rate of dissociation of internally excited molecules. A previously determined model for collision-induced dissociation is tested by comparison of predicted and experimentally observed orifice–skimmer potential differences for dissociation of ions. The rate of collision-induced dissociation of bradykinin ions is determined by monitoring the fragments produced in a mass spectrometer. The semi-quantitative model is found to yield effective predictions when accurate Arrhenius and RRK parameters are utilized. (J Am Soc Mass Spectrom 2001, 12, 772-779) © 2001 American Society for Mass Spectrometry

Electrospray ionization (ESI) is a soft ionization technique that is easy to operate and applicable to most types of solutions. It has numerous applications when coupled with mass spectrometry (MS), including the analysis of proteins [1–6], nucleotides [7–9], and other compounds [10–12]. It is commonly coupled with continuous types of mass analyzers such as quadrupoles [13–15], but is also effective for pulsed mass analyzers, such as time-of-flight [16, 17], and ion traps [18–21].

By increasing the potential difference between the orifice and the skimmer of a mass spectrometer designed for ESI-MS, ions from the source are accelerated through this region, and acquire increased internal energy through collisions with the background gas molecules. The increase in internal energy is proportional to the potential difference between the orifice and the skimmer, and therefore, the energy deposited in an ion can be controlled. The main disadvantage of this technique is that ions are not mass selected prior to fragmentation. All of the components of a sample experience the same conditions within the orifice–skimmer region, and this leads to complicated fragmentation spectra when complex mixtures are analyzed. However, this problem can be alleviated by combining a separation technique, such as capillary electrophoresis or high performance liquid chromatography (HPLC), with ESI-MS. An equation was derived recently to describe the variation in the gas number density as gas expands from atmospheric pressure through an orifice into the first stage of a vacuum system of an ESI-MS [22]. This equation enabled us to semi-quantitatively predict the orifice voltages necessary to fragment various cyclodextrin ions generated by electrospray ionization. However, due to the difficulties in determining an accurate vibrational frequency and the effective number of degrees of freedom for the cyclodextrin analysis using RRK theory, it is necessary to explore other models for unimolecular dissociation.

Bradykinin, a nonapeptide important in the human body's response to trauma, is chosen for this study because it has been extensively studied in the gas phase. The Arrhenius pre-exponential factor and activation energy have been determined by blackbody infrared radiative dissociation (BIRD) [23, 24] and thermal dissociation [25]. Its gas phase conformation, and the efficiency of transfer of center of mass energy into internal energy have been determined [26, 27]. The purpose of this paper is to further test the previously developed model [22] using both the Arrhenius equation and RRK theory to predict the rates of dissociation of bradykinin within the interface region of three different electrospray ionization mass spectrometers.

Experimental

Chemicals and Apparatus

The acetate salt of bradykinin of 99% purity was from Sigma (St. Louis, MO). HPLC grade methanol and glacial acetic acid were from Fisher Scientific Ltd (Nepean, Ont.). The sample was prepared by dissolving the bradykinin salt in a solution of 59.5% water, 39.5% methanol, and 1% acetic acid, at a concentration of 10^{-4} M.

Published online May 4, 2001
Address reprint requests to Dr. David D. Y. Chen, Department of Chemistry, University of British Columbia, 2036 Main Mall, Vancouver, BC, V6T 1Z1, CN. E-mail: chen@chem.ubc.ca

1044-0305/01/$20.00
PII S1044-0305(01)00266-5

Received November 27, 2000
Revised March 9, 2001
Accepted March 9, 2001

The instruments used for this study were a prototype single quadrupole ionspray mass spectrometer and a prototype triple quadrupole ionspray mass spectrometer from SCIEX (Thornhill, Ontario, Canada), and a linear ion trap time of flight mass spectrometer (LIT-TOF-MS) constructed in-house by the Don Douglas research group [17]. For the two quadrupole systems, a reduced flow (0.2 μL/min) electrospray ion source was used [22, 28]. The tapered spray tips were pulled in-house, and had an internal diameter at the tip of approximately 20 μm. A voltage of 3 kV was applied for electrospray with a constant curtain gas flow of approximately 1 L/min as measured by a series FM-1050 gas flow meter (Matheson, Montgomeryville, PA). Medical grade nitrogen from Praxair (Mississauga, Ontario, Canada) was used as the curtain gas for both quadrupole systems, and ultra high purity nitrogen from Praxair (Mississauga, Ont.) for the LIT-TOF-MS. A syringe pump (Harvard Apparatus Syringe Infusion Pump 22, South Natick, MA) was used to generate a solution flow rate of 0.2 μL/min. For the LIT-TOF-MS an ionspray source was used with an electrospray potential of 5000 V. The solution flow rate was 1 μL/min, and the nebulizer gas pressure was maintained at 15 psi.

Results and Discussion

A free jet is formed when a gas expands into vacuum through the sampling orifice of an electrospray ionization mass spectrometer. The enthalpy of the gas is converted into directed bulk flow kinetic energy, and the local temperature of the gas decreases as shown in the following equation [29]:

$$T = T_0(1 + 0.5(\gamma - 1)M^2)^{-1} \quad (1)$$

where, T is the temperature at a given point in the free jet, T_0 is the source temperature, γ is the ratio of heat capacity at constant pressure to heat capacity at constant volume (C_p/C_v), and M is the local Mach number, which is the ratio of the gas flow speed to the local speed of sound. Within the gas expansion, the Mach number is given by [30]:

$$M = A\left(\frac{x - x_0}{D}\right)^{\gamma-1} - \frac{1}{2}\left(\frac{\gamma + 1}{\gamma - 1}\right)\Big/A\left(\frac{x - x_0}{D}\right)^{\gamma-1} \quad (2)$$

where A and x_0 are constants that are dependant on the value of γ, D is the orifice diameter, and x is the distance downstream from the orifice. The values of A and x_0 used in this study were 3.65 and 0.40 D respectively [30], and the orifice diameter for the instruments used in this study was measured to be approximately 0.25 mm. For nitrogen, a Mach number of one is achieved within approximately 72% of an orifice diameter. The gas number density at this point in the free jet has dropped to 66.8% of that at atmospheric pressure.

For the two quadrupole mass spectrometers, we have previously shown that the skimmer is located prior to the calculated position of the mach disk, where the disturbance at the end of a free jet causes the temperature of the gas to rise to approximately the temperature of the source region [22]. The distance between the orifice and the skimmer is 1.7 mm for the single quadrupole instrument, 2.1 mm for the LIT-TOF-MS, and 3 mm for the triple quadrupole mass spectrometer.

The gas number density along any streamline of the free jet expansion between the orifice and the skimmer of the mass spectrometers, with nitrogen as the curtain gas, ($\gamma = 1.4$) is given by [22]:

$$n_i = \frac{n_0}{\left(2.6645(39.2157x - 0.4)^{0.8} + \frac{0.1351}{(39.2157x - 0.4)^{0.8}} - 0.2\right)^{2.5}} \quad (3)$$

where n_i is the gas number density at some point within the free jet, n_0 is the gas number density in the source region (2.5 E19 cm^{-3}), and x is the distance from the orifice. Within a free jet expansion, the gas density drops off with roughly an inverse square relationship to the distance from the orifice. The free jet forms at a distance of 0.0142 cm from the orifice.

In order to determine the number of collisions occurring within this region, it is necessary to calculate the mean free path for bradykinin ions in the laboratory frame of reference, λ, by [22]:

$$\lambda = \frac{1}{n\sigma}\left(1 + \frac{v}{c}\right) \quad (4)$$

where n is the number density, σ is the collision cross section for the ion and the target gas molecule, v is the velocity of the expansion gas flow, and c is the velocity of the ion in the gas frame of reference.

The cross section for the collisions between bradykinin and nitrogen was calculated by:

$$\sigma = \pi(r_1 + r_2)^2 \quad (5)$$

where r_1 and r_2 are the cross sectional radii of protonated bradykinin and nitrogen respectively. The radius of a diatomic nitrogen gas molecule was estimated to be 1.49 angstroms from its covalent radius [22], and the diameter of protonated bradykinin was estimated to be 16.57 angstroms. The diameter of protonated bradykinin was estimated from eq 5 and the work of Wytten-

bach et al., who accurately determined the collision cross sections for singly- and multiply-charged bradykinin colliding with helium [26]. The collision cross section used for this study was 301 Å^2. This cross section was assumed to remain constant throughout the region between the orifice and the skimmer. In reality, ions become desolvated as they travel through the region, so the collision cross section would probably not be constant throughout.

A spreadsheet was generated using Microsoft Excel 2000 to model the collisions between bradykinin and nitrogen. As previously mentioned, the origin of the free jet was taken as 0.0142 cm from the orifice. The mean free path for a bradykinin ion was calculated at this point using eq 4 to determine how far the peptide would accelerate along a streamline in the free jet prior to a collision. This mean free path was then added to the initial position to yield the start of the next segment in the free jet. The number density and the mean free path were calculated again for this point using eqs 3 and 4 to determine the linear distance from the orifice where the second collision would occur. This process was repeated for the entire distance between the orifice and the skimmer. The calculated number of collisions ranged from 158 to 2762 for singly protonated bradykinin when the orifice–skimmer voltage is varied from 0 to 250 V in the triple quadrupole mass spectrometer. The total number of collisions was found to be slightly higher for the single quadrupole mass spectrometer and the LIT-TOF-MS at the same orifice voltages, even though the orifice–skimmer spacing is smaller on both of these systems. This is due to the increased electric field generated within the orifice–skimmer region of the single quadrupole and the LIT-TOF-MS causing the velocity of an ion in the gas frame of reference to increase substantially, decreasing the laboratory mean free path.

Collisions between bradykinin ions and the neutral gas molecules convert the ion translational energy into internal energy of the bradykinin ions. The center of mass coordinate system was used to model the energy conversion in these collisions [31]. The kinetic energy of an ion prior to the (i)th collision, ($E_{i,\mathrm{gas}}$), which is also its translational energy in the gas frame of reference is described by:

$$E_{i,gas} = E'_{i-1,gas} + q\Delta V \tag{6}$$

where $E'_{i-1,\mathrm{gas}}$ is the ion translational energy after the ($i-1$)th collision, q is the charge on the ion, and ΔV is the potential difference that the ion is accelerated through. It is important to note that in the laboratory frame of reference, the kinetic energy of the ion is slightly higher (by a factor of v_{flow}). This factor contributes equally to both the energy of the bradykinin ions and the energy of the neutral gas molecules, so it is important to model the collisions in the gas frame of reference. The energy available for conversion to internal energy of the ion is the center of mass energy given by [31]:

$$E_{cm} = \frac{m_2}{m_1 + m_2} E_{gas} \tag{7}$$

where m_2 is the mass of the target gas molecule, and m_1 is the mass of the ion. The center of mass energy was determined for each collision. All collisions were treated as inelastic involving a moving ion and a stationary gas molecule. Marzluff et al. have demonstrated from trajectory calculations that greater than 90% of the calculated center of mass energy was converted into internal energy of bradykinin [27]. Recent studies suggest that this conversion is slightly less efficient when averaged over all impact parameters and peptide orientations [32, 33]. For these studies, a 90% conversion rate of center of mass energy into internal energy was assumed.

The ratio of the kinetic energy of an ion after and before an inelastic collision with a stationary gas molecule is given by [22]:

$$\frac{E'_{gas}}{E_{gas}} = \frac{m_1^2}{m^2} \tag{8}$$

where E'_{gas} and E_{gas} are the translational energy of the ion in the gas coordinate system after and before a collision, and m is the sum of the masses of the ion and the gas molecule. This equation accounts for translational energy losses due to conversion of E_{cm} to internal energy of the ion, as well as recoil of the neutral gas molecule [34]. Equation 8 was used to determine that approximately 95% of the translational energy of the bradykinin ions was maintained after each of the collisions. The calculated ion translational energy after the collision (E'_{gas}) was then used as the new initial translational ion energy at the start of the next single collision region on the spreadsheet. The total energy converted to internal energy of the bradykinin ions was determined by summing the contributions from all of the collisions with nitrogen. These calculations were carried out at various orifice–skimmer potential differences to yield a working curve of ion internal energy versus orifice–skimmer potential difference. This working curve allows us to predict the necessary orifice voltage to fragment ions with various bond strengths. Figure 1 illustrates a plot of the kinetic energy converted to internal energy at various distances from the orifice on the single quadrupole mass spectrometer. The free jet region is divided into 80 μm segments to illustrate that similar amounts of internal energy are generated in all regions of the free jet expansion. In the first region, over a thousand low energy collisions occur, at an orifice–skimmer potential difference of 100 V, which impart the same internal energy as the 5 or 6 high energy collisions in the final region. The difference in energy between these collisions is due to the larger

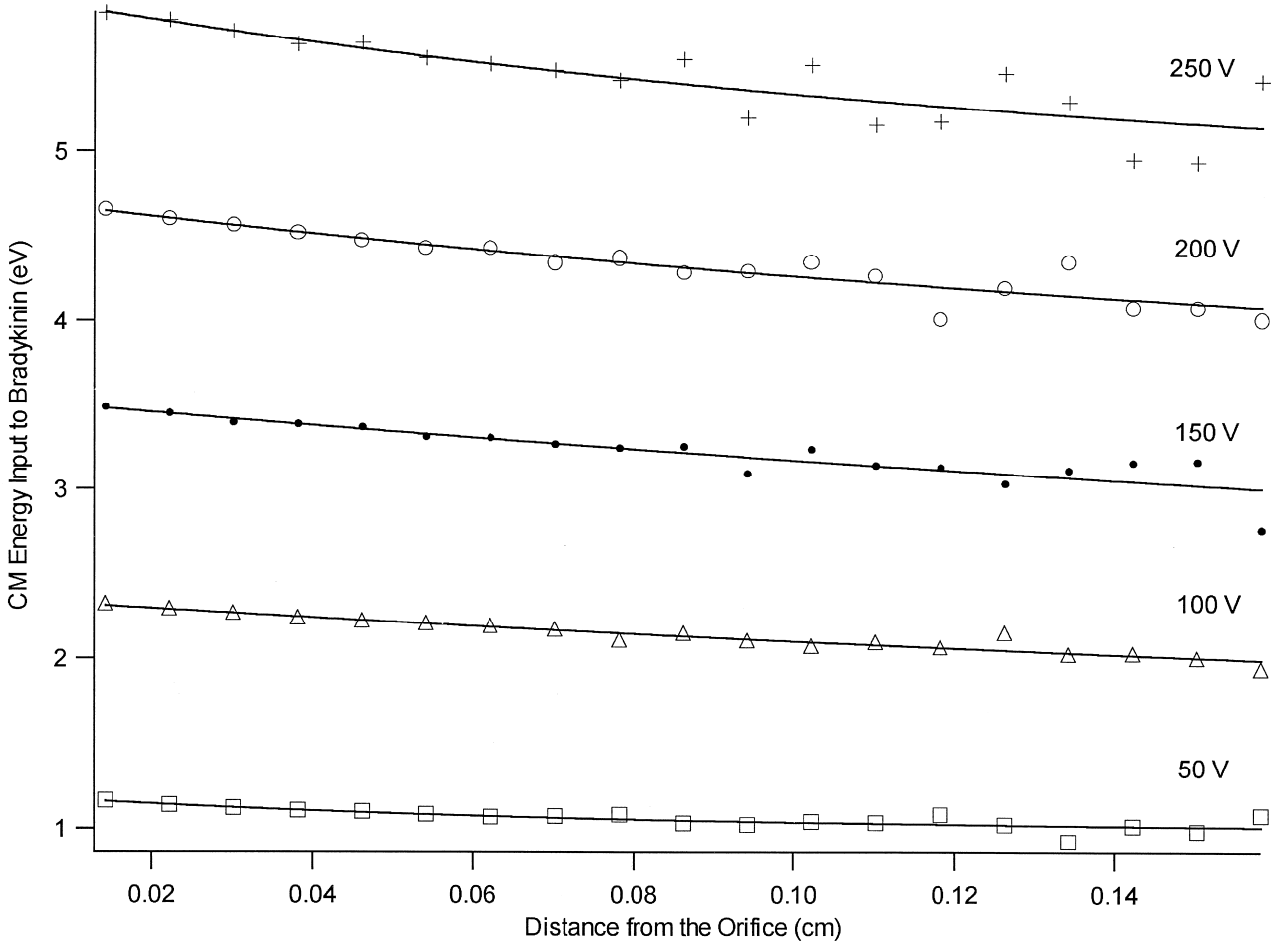

Figure 1. Center of mass energy converted to internal energy of bradykinin ion per 80 μm region from the origin of the free jet on the single quadrupole mass spectrometer. The data for orifice–skimmer voltage differences of 250, 200, 150, 100, 50, and 0 V are illustrated.

mean free path for ion acceleration close to the skimmer.

Two different methods were used in this study to determine the internal energy necessary for dissociation of bradykinin molecules. Method one involved the Arrhenius equation with activation energies and pre-exponential factors determined from BIRD experiments. For unimolecular dissociation of singly protonated bradykinin, the pre-exponential factor is 10^{12} s^{-1} and the activation energy is 1.3 eV [23, 24]. Although these values are measured in the zero-pressure limit, they can be applied to the interface region of an electrospray mass spectrometer for large molecules. Large biomolecules absorb and emit blackbody radiation at a rate much higher than the rate of dissociation. In this regime, where the internal energy distribution of the biomolecule can be characterized by a Boltzmann distribution, the pre-exponential factor and activation energy determined by BIRD approach the values of the high pressure limit [35, 36]. Simple first order kinetics was used to predict the necessary rate constant for bond dissociation on the order of the time frame for the bradykinin ions to travel through the mass spectrometers. The equation for this is the following:

$$\ln \frac{[A]}{[A_0]} = -kt \tag{9}$$

where $[A]$ is the concentration of the parent ion at time t, $[A_0]$ is the initial parent ion concentration, and k is the unimolecular rate constant. This equation was used to determine the rate constant necessary for 10% dissociation of the bradykinin ions. The calculated rate constant was 105.4 s^{-1} assuming that it takes approximately 1 ms for an ion to travel from the skimmer to the mass analyzer of the mass spectrometers. The Arrhenius equation was used to determine the necessary ion internal temperature to generate this unimolecular reaction rate constant. The equation is given by [37]:

$$k = Ae^{-Ea/RT} \tag{10}$$

where k is the rate constant, A is the pre-exponential factor, Ea is the activation energy, R is the gas constant, and T is the temperature. Utilizing the rate constant calculated above, the necessary internal temperature was calculated to be 656 K. To determine the amount of energy needed to heat the ions to this temperature, it is assumed that the ion internal temperature was equilibrated to room temperature, or 295 K, prior to heating within the orifice–skimmer region. Thus, the temperature difference is 361 K. Assuming most of the internal energy of the ion is present as vibrational energy, the internal energy necessary to achieve 10% dissociation is estimated by:

$$\Delta E = nk\Delta T \tag{11}$$

where n is the number of degrees of freedom, k is the Boltzmann constant, and ΔT is the temperature change. For the singly charged bradykinin ion, it was estimated that 13.83 eV of internal energy is necessary to cause a 10% fragmentation of the ion within the mass spectrometers. Integration of the heat capacity of bradykinin as a function of temperature would be required if a more accurate energy is needed.

The second method used to predict the internal energy requirement to achieve fragmentation of bradykinin ions was the RRK equation, given by [38]:

$$K \approx v\left(\frac{E - E_0}{E}\right)^{s-1} \tag{12}$$

where K is the RRK rate constant for unimolecular dissociation of the activated complex, ν is a vibrational frequency, E is the ion internal energy, E_0 is the bond strength, and s is the number of vibrational degrees of freedom. It has been found that the results obtained from eq 12 are closer to experimental results when a decreased number of vibrational degrees of freedom is used [38]. For calculations with the RRK theory, the number of degrees of freedom was reduced by a factor of 3. Bradykinin has 150 atoms, and thus has 444 internal degrees of freedom. The threshold dissociation energy was 2.5 eV for bradykinin [39], and the RRK rate constant was 10^2 to reflect a 10% dissociation on the time scale of the ions travel from the skimmer to the mass analyzer. The vibrational frequency used in this study was $10^{13.2}$ s^{-1} [27, 39]. Using this equation, the ion internal energy necessary to yield a 10% ion fragmentation ratio in the mass spectrometers is 13.72 eV. It is important to note that RRKM theory is generally a more satisfactory method for determining kinetic shifts, but when proper values are used, RRK theory and the arrhenius equation have been shown to produce similar results [40].

The mass spectra of 10^{-4} M bradykinin solution shows the presence of singly, doubly, and triply protonated ions, identified by resolving the isotopic peak spacing. To determine the fragments observed for each of these ions, the triple quadrupole mass spectrometer was first used to conduct tandem mass spectrometry. Each ion was separately mass selected in Q1, followed by collisional activation in Q2. The fragments were then observed by scanning a wide range of masses in Q3.

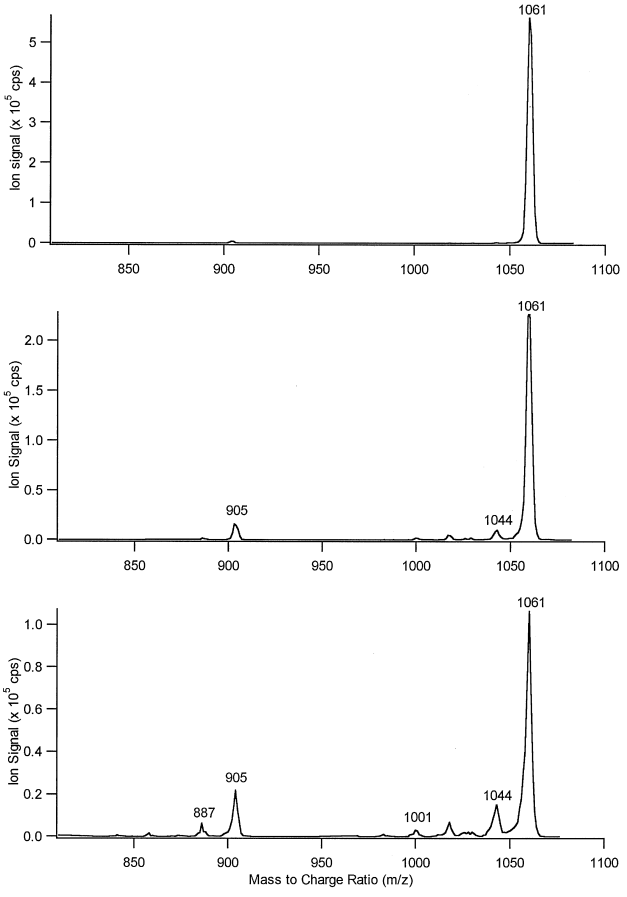

Figure 2. Fragment ion spectra of singly protonated bradykinin at varying ion energies in the triple quadrupole mass spectrometer. The ion energy ranges from 51 eV to 161 eV, and the main daughter peaks observed correspond to b_8^+ (m/z = 887), y_8^+ (m/z = 905), $(P+H-NH_3)^+$ (m/z = 1044), and $(P+H-60)^+$ (m/z = 1001).

The MS/MS spectra of the triply protonated bradykinin ions contains peaks corresponding to $(P+3H)^{3+}$, $(P+3H-H_20)^{3+}$, y_2^+, b_4^+, y_3^+, y_4^+, b_5^+, $(P+2H)^{2+}$ and other fragments as described using the notation of Roespstorff [41]. Fragments from the triply charged ion include the doubly protonated bradykinin, making it difficult to quantitatively determine the behavior of the doubly charged peak as the orifice–skimmer potential is increased. For this reason, and because the doubly charged peak was observed to exhibit extensive fragmentation, only the singly protonated bradykinin molecule was used for calculations in this study.

The results obtained for MS/MS of singly protonated bradykinin with the triple quadrupole mass spectrometer are shown in Figure 2 with 1 mTorr of nitrogen in Q2. The ion translational energy prior to Q2 is 51 eV, 101 eV, and 161 eV, respectively. At low energies, the singly charged ion fragments to yield predominantly

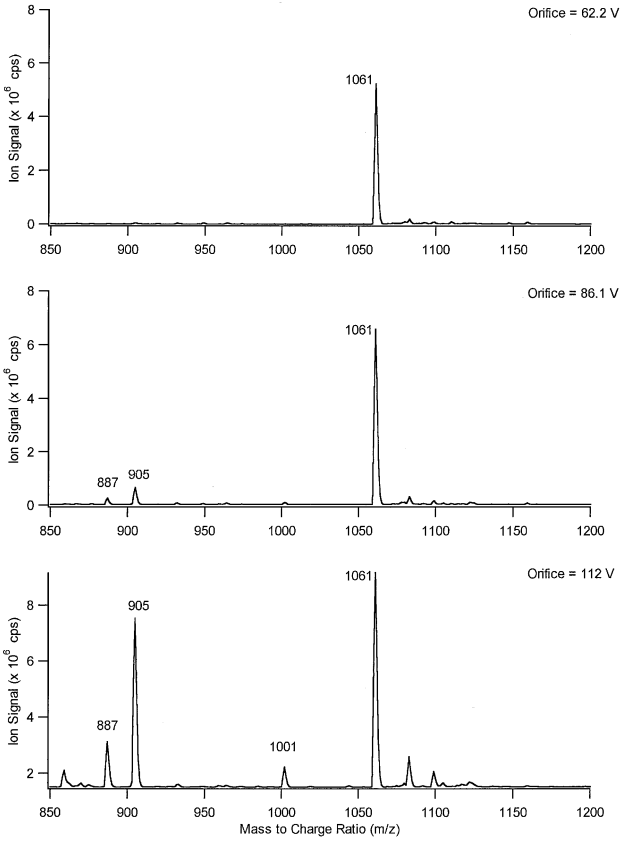

Figure 3. Fragmentation spectra of singly protonated bradykinin (m/z = 1061) obtained utilizing various potential differences (62, 86, and 112 V) between the orifice and the skimmer of the single quadrupole mass spectrometer. The main fragment ion peaks correspond to b_8^+ (m/z = 887), y_8^+ (m/z = 905), and $(P+H-60)^+$ (m/z = 1001).

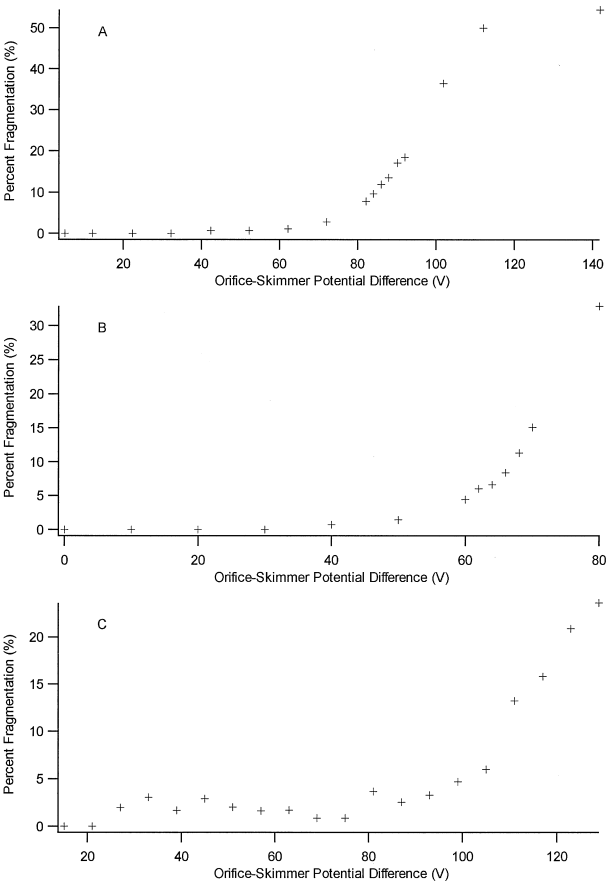

Figure 4. Percent fragmentation of singly protonated bradykinin with an increase in the orifice–skimmer potential difference on the single quadrupole (**a**), triple quadrupole (**b**), and LIT-TOF (**c**) mass spectrometers.

the y_8^+ fragment. At higher fragmentation energies, the b_8^+ peak and the $(P+H-NH_3)^+$ peak become evident as well as a peak corresponding to $(P+H-60)^+$.

Utilizing the potential difference between the orifice and the skimmer of the three mass spectrometers, the predominant fragments observed for singly protonated bradykinin are the y_8^+ fragment and the b_8^+ fragment. At higher orifice–skimmer potential differences, the $(P+H-60)^+$ fragment was observed. The sum of the fragments was used to determine the extent of fragmentation of the parent peak. The skimmer was maintained at ground on the single quadrupole mass spectrometer, 110 V on the triple quadrupole mass spectrometer, and 15 V on the LIT-TOF-MS. Typical data for orifice–skimmer dissociation of the singly charged bradykinin ions is shown in Figure 3 for the single quadrupole mass spectrometer. The orifice potentials were 62.2, 86.1, and 112 V for the three runs respectively. The fragments produced by collision-induced dissociation (CID) in the interface region are similar to those in Q2. This similarity has been noted previously for other peptides [42, 43], however for proteins, the formation of dimers and multimers in the source can make direct comparisons difficult [44]. A significantly higher degree of ion fragmentation can occur when ions are heated within the orifice–skimmer region. The fragmentation in Q2 can be increased with higher collision gas pressures and ion translational energy.

The orifice–skimmer fragmentation curves for the single quadrupole (a), triple quadrupole (b), and LIT-TOF-MS (c) are shown in Figure 4. Each of the points represents an average of three replicates. The fragmentation curves were reproducible, with a relative standard deviation of approximately 5% for each measurement taken at the 10% dissociation level. The curves look very similar for the three instruments, demonstrating an increase in the degree of fragmentation occurring approximately 20 V after desolvation of the ions. Typical orifice–skimmer potential differences used to achieve desolvation were 30 V, 50 V, and 70 V for the triple quadrupole [22], single quadrupole [22], and time of flight mass spectrometers respectively. Ions can be heated very rapidly between the orifice and the skimmer of an ESI-MS. The heated ions then enter the Q0 region of the instrument, where collisional cooling occurs. In this region, the ions gain a small amount of internal energy from the collisions with the gas molecules, but also lose a small amount of internal energy

Table 1. Predicted and observed orifice voltages for 10% dissociation of protonated bradykinin in three different mass spectrometers

Instrument	Predicted voltage using the Arrhenius equation with BIRD values (V)	Predicted voltage using the RRK equation (V)	Observed orifice voltages (V) (±2V)
Single Quadrupole Mass Spectrometer	86	86	85
Triple Quadrupole Mass Spectrometer	177	177	177
Linear Ion Trap-Time of Flight-Mass Spectrometer	121	121	123

via collisional deactivation and emission of radiation. The rate of input of internal energy to the ions between the skimmer and Q0 was minimized by maintaining a small potential difference of 7 V between them. Losses of internal energy due to radiative relaxation were assumed to be negligible because of the short time scale of these experiments (≈1 ms). The LIT-TOF-MS was found to require a larger desolvation energy than either of the two quadrupole instruments. This is most likely due to the fact that the gas pressure within Q0 of the LIT-TOF-MS (1.8 mTorr) is lower than it is in the quadrupole systems (7 mTorr). As a result, an ion experiences fewer collisions to maintain its internal temperature within Q0, necessitating an increased orifice–skimmer voltage difference. Another possible reason for the large orifice–skimmer voltage difference necessary for desolvation may be the larger droplet size formed by the ionspray ionization source as opposed to the reduced flow ionization source. This may cause the ions to enter the mass spectrometer with a higher degree of solvation.

The predicted orifice voltages for fragmentation of the singly protonated bradykinin on the single and triple quadrupole mass spectrometers, and the LIT-TOF-MS are compared with the experimental results in Table 1. The predictions by RRK theory and the Arrhenius equation are in agreement, and are similar to what is observed experimentally. The predictions are accurate for all three instruments, demonstrating the general applicability of this model.

The RRK equation is based upon a micro canonical theory that can be used to determine a kinetic shift for large biomolecules. The rate constant for unimolecular dissociation obtained is independent of the method of ion excitation. To achieve a reasonable estimate for internal energy requirements using this theory, it is crucial to use correct values for the rate constant, the number of degrees of freedom, and the vibrational frequency of the molecule. A variation of either the vibrational frequency or the RRK rate constant by a factor of 10 for this molecule varies the predicted internal energy requirement by 9.3%. Decreasing the number of degrees of freedom by a factor of 4 rather than 3 results in an 11.95% decrease in the calculated internal energy to 12.08 eV. This is a 1.6 eV decrease in internal energy, but only varies the predicted dissociation voltage by 4 V. The variability of these parameters makes it difficult to use RRK theory for ions which have not been extensively studied. However, for well characterized ions such as bradykinin, these uncertainties result in minimal difference in the predicted orifice–skimmer potential difference.

When adjusting the orifice–skimmer potential difference to achieve fragmentation in ESI-MS, it is extremely uncommon to vary the potential difference by an increment smaller than 5 V. Therefore, a semi-quantitative model for unimolecular dissociation is useful if it can predict potential differences to within approximately 5–10 V. Due to the rapid increase in fragmentation near the dissociation threshold energy, the calculated error in the predicted orifice voltages for dissociation is approximately 2 V. These results support the premise that ions are heated in a series of collisions in the interface region in ESI-MS, and the total internal energy acquired by an ion can be regarded as the sum of the energy generated in each of the individual ion/neutral collisions. Further evaluation of this model is necessary to determine its general applicability.

Conclusion

This work demonstrates that the rate of unimolecular dissociation of ions can be predicted based upon the internal energy an ion acquires through collisions with background gas molecules, and that the magnitude of the acquired energy can be controlled by adjusting the orifice–skimmer potential difference on an electrospray ionization mass spectrometer. Predicted values for 10% dissociation of bradykinin are similar to the experimental values when either the Arrhenius equation or RRK theory is used. Useful predictions by either method require knowledge of appropriate values including the threshold dissociation energy, vibrational frequency, number of vibrational degrees of freedom, Arrhenius preexponential factor, and activation energy. Useful predictions are made for bradykinin when the degree of fragmentation is chosen to be below approximately 20% because extensive fragmentation at higher energies makes it difficult to unambiguously assign the daughter peaks to the singly charged parent ion.

Acknowledgments

The authors thank Dr. Bruce Collings for insightful discussions and technical assistance. This work is supported by the Natural Sciences and Engineering Research Council of Canada (NSERC), and Applied Biosystems/MDS SCIEX. B.B.S. acknowledges a post-graduate scholarship from NSERC.

References

1. Figeys, D.; Aebersold, R. *Electrophoresis.* **1997,** *18*, 360.
2. Carbeck, J. D.; Severs, J. C.; Gao, J.; Wu, Q.; Smith, R. D.; Whitesides, G. M. *J. Phys. Chem. B.* **1998,** *102*, 10596.
3. Konermann, L.; Collings, B. A.; Douglas, D. J. *Biochem.* **1997,** *36*, 5554.
4. Fridriksson, E. K.; Baird, B.; McLafferty, F. W. *J. Am. Soc. Mass Spectrom.* **1999,** *10, 453.*
5. Wilm, M.; Shevchenko, A.; Houthaeve, T.; Brelt, S.; Schweigerer, L.; Fotsis, T.; Mann, M. *Nature.* **1996,** *379*, 466.
6. Loo, J. A. *Mass Spectrom. Rev.* **1997,** *16*, 1.
7. Cheng, X.; Gale, D. C.; Udseth, H. R.; Smith, R. D. *Anal. Chem.* **1995,** *67*, 586.
8. Bayer, E.; Bauer, T.; Schmeer, K.; Bleicher, K.; Maier, M.; Gaus, H. J. *Anal. Chem.* **1994,** *66*, 3858.
9. Strittmatter, E. F.; Schnier, P. D.; Klassen, J. S.; Williams, E. R. *J. Am. Soc. Mass Spectrom.* **1999,** *10*, 1095.
10. Weinmann, W.; Wiedemann, A.; Eppinger, B.; Renz, M.; Svoboda, M. *J. Am. Soc. Mass Spectrom.* **1999,** *10*, 1028.
11. Desaire, H.; Leary, J. A. *Anal. Chem.* **1999,** *71*, 4142.
12. Sun, W.; Cui, M.; Liu, S.; Song, F.; Elkin, Y. N. *Rapid Commun. Mass Spectrom.* **1998,** *12*, 2016.
13. Smith, R. D.; Loo, J. A.; Barinaga, C. J.; Edmonds, C. G.; Udseth, H. R. *J. Am. Soc. Mass Spectrom.* **1990,** *1*, 53.
14. Mansoori, B. A.; Volmer, D. A.; Boyd, R. K. *Rapid Commun. Mass Spectrom.* **1997,** *11*, 1120.
15. Konermann, L.; Douglas, D. J. *Biochem.* **1997,** *36*, 12296.
16. Cao, P.; Moini, M. *J. Am. Soc. Mass Spectrom.* **1998,** *9*, 1081.
17. Campbell, J. M.; Collings, B. A.; Douglas, D. J. *Rapid Commun. Mass Spectrom.* **1998,** *12*, 1463.
18. Figeys, D.; Ning, Y.; Aebersold, R. *Anal. Chem.* **1997,** *69*, 3153.
19. Gross, D. S.; Zhao, Y.; Williams, E. R. *J. Am. Soc. Mass Spectrom.* **1997,** *8*, 519.
20. Li, W.; Hendrickson, C. L.; Emmett, M. R.; Marshall, A. G. *Anal. Chem.* **1999,** *71*, 4397.
21. Juraschek, R.; Dulcks, T.; Karas, M. *J. Am. Soc. Mass Spectrom.* **1999,** *10*, 300.
22. Schneider, B. B.; Chen, D. D. Y. *Anal. Chem.* **2000,** *72*, 791.
23. Price, W. D.; Schnier, P. D.; Williams, E. R. *Anal. Chem.* **1996,** *68*, 859.
24. Schnier, P. D.; Price, W. D.; Jockush, R. A.; Williams, E. R. *J. Am. Chem. Soc.* **1996,** *118*, 7178.
25. Butcher, D. J.; Asano, K. G.; Goeringer, D. E.; McLuckey, S. A. *J. Phys. Chem. A*, **1999,** *103*, 8664.
26. Wyttenbach, T.; von Helden, G.; Bowers, M. T. *J. Am. Chem. Soc.* **1996,** *118*, 8355.
27. Marzluff, E. M.; Campbell, S.; Rodgers, M. T.; Beauchamp, J. L. *J. Am. Chem. Soc.* **1994,** *116*, 6947.
28. Figeys, D.; Aebersold, R. *Electrophoresis.* **1997,** *18*, 360.
29. Douglas, D. J. In *Inductively Coupled Plasmas in Analytical Atomic Spectrometry, 2nd ed.*; Montaser, A.; Golightly, D. W., Eds.; VCH Publishers: New York, 1992; pp 613–650.
30. Ashkenas, H.; Sherman, F. S. In *Fourth International Symposium on Rarefied Gas Dynamics* Vol. II; Deleeuw, J. H., Ed.; Academic Press: New York, 1965; pp 84–105.
31. Douglas, D. J. *J. Am. Soc. Mass Spectrom.* **1998,** *9*, 101.
32. Meroueh, O.; Hase, W. L. *J. Phys. Chem.* **1999,** *103*, 3981.
33. Meroueh, O.; Hase, W. L. *Intl. J. Mass Spectrom.* **2000,** *201*, 233.
34. Covey, T.; Douglas, D. J. *J. Am. Soc. Mass Spectrom.* **1993,** *4*, 616.
35. Price, W. D.; Schnier, P. D.; Jockusch, R. A.; Strittmatter, E. F.; Williams, E. R. *J. Am. Chem. Soc.* **1996,** *118*, 10640.
36. Price, W. D.; Williams, E. R. *J. Phys. Chem. A.* **1997,** *101*, 8844.
37. Zumdahl, S. S. *Chemical Principles*; D.C. Heath and Company: Lexington, MA, 1992; p 672.
38. Laidler, K. J. *Theories of Chemical Reaction Rates*; McGraw-Hill Publishers: New York, 1969; p 119.
39. Marzluff, E. M.; Beauchamp, J. L. In *Large Ions: Their Vaporization, Detection and Structural Analysis*; John Wiley & Sons Ltd: New York, 1996; p 115–143.
40. Bernschtein, V.; Oref, J. *J. Phys. Chem.* **1994,** *98*, 136.
41. Roepstorff, P.; Fohlman, J. *J. Biomed. Environ. Mass Spectrom.* **1984,** *11*, 601.
42. Harrison, A. G. *Rapid Commun. Mass Spectrom.* **1999,** *13*, 1663.
43. Van Dongen, W. D.; Van Wijk, J. I. T.; Green, B. N.; Heerma, W.; Haverkamp, J. *Rapid Commun. Mass Spectrom.* **1999,** *13*, 1712.
44. Thomson, B. A. *J. Am. Soc. Mass Spectrom.* **1997,** *8*, 1053.